Fabrication of Ceramic-Metal Functionally Graded Materials

Dr. Alaa A. Atiyah
Material Engineering Department, University of Technology, Baghdad
Dr. Saad. B. H. Farid
Material Engineering Department, University of Technology, Baghdad
Dheya N. Abdulamer
Center of Energy and Fuel researches, University of Technology, Baghdad

Received on: 15/5/2012 & Accepted on: 6/9/2012

ABSTRACT

High order step wise functionally graded materials Al_2O_3-Ti are fabricated. These materials combine the high fracture toughness of Ti phase and the relatively low density of Al_2O_3 and stand for candidate materials for harsh mechanical and thermal environments. The techniques of powder technology are utilized to fabricate these materials that composed of five graded layers of Al_2O_3-Ti phases. Al_2O_3 increasing linearly across these layers (0, 25, 50, 75 and 100wt% respectively).

The green specimens are composed of Al_2O_3-TiH_2 layers and the sintered specimens are composed of graded Al_2O_3-Ti. Spark Plasma Sintering technique is utilized for sintering of the graded green specimens. The best sintering conditions is found at 1500°C for 30 minute of sintering that gives apparent density of 4.25 g/cm^3, porosity of 1.28% and diametric expansion of 1.58%. Optical microscopy shows gradual transition of phases at the interface of the graded layers.

Keywords: Functionally graded materials, Spark plasma sintering.

تحضير المواد المتدرجة وظيفيا لـــ (سيراميك – فلز)

الخلاصـــــــــة

تم تصينع مواد متدرجة من **Al_2O_3-Ti** بطبقات متسلسلة عديدة. تجمع هذه المـــواد بـــين مقاومـــة الكســـر العالية لطور **Ti** والكثافة المنخفضة نسبيا لطور **Al_2O_3** وترشح هذه المواد كمواد منافســـة في الظروف الميكانيكية والحرارية القاســـية. تم استخدام تقنيات المساحيق لتصنيع هذه المواد والمؤلفة مـــن خمســـــة طبقات متدرجة بنسب الاطوار **Al_2O_3-Ti**. تتزايد نســـــبة الطـــور **Al_2O_3** خطيـــا خـــلال الطبقات (**0**، **25**، **50**، و **100wt%** على التوالي).

تتكون النماذج الخضراء من طبقات من **Al_2O_3-TiH_2** وتكون النماذج بعد التلبيد مكونة من تـــدرج من **Al_2O_3-Ti**. تم تلبيد النماذج المتدرجة الخضراء باستخدام التلبيد بشرارة البلازما. ووجد ان أفضـــل ظروف للتلبيد هي في درجة حرارة التلبيد **1500°C** لزمن تلبيـــد **30** دقيقـــة والـــذي ادى الـــى كثافـــة ضاهرية بمقدار **4.25 g/cm^3** ومســـــــامية بمقدار **1.28%** وتمدد قطري بمقـــدار **1.58%**. وقـــد اظهرت فحوصات المجهر الضوئي تحول متدرج للاطوار على الحدود بين الطبقات المتدرجة.

INTRODUCTION

Much research and development have been carried out to develop Functionally Graded Materials FGMs for various applications using gradients in physical, chemical, biochemical, and mechanical properties. The main characteristic that distinguishes FGMs from conventional composite materials is the tailoring of graded composition and microstructure in an intentional manner. That gradation aimed to design the distribution of properties needed to achieve the desired function. The majority of FGMs design case the integration of incompatible functions of the refractoriness and wear resistance of ceramics in one side and the toughness of metals on the other side; which found various structural applications [1].

FGM_s that are made from a mixture of metal and ceramics are typically characterized by smooth and continuous change of the mechanical properties from one side to another. These FGM_s designs are reported to overcome weakness of the laminated composite materials; such as de-bonding at massive stress or local large plastic deformations [2].

Another case study is the fabrication of metal-ceramic joints; where cracking are often occurs during the buildup of residual stresses caused by the large difference in thermal expansion between metal and ceramic components. FGM designs proofs excellent solution in such cases as a result of the spatial variation in composition. That gradation in composition keeps the thermo-mechanical stresses within acceptable limits and minimizes the residual thermal stresses [3].

Generally, the compositional gradient obtainable by the functionally graded materials FGM_s offer a solution for problems arises from the existence of sharp interfaces by tolerating continuous transition from one material property to the another property avoiding abrupt mismatch [4].

Nevertheless, the synthesis if a gradient material is a challenge itself. A process design stage should be accomplished for synthesis of gradient material. Thus, a wide variety of available processes have been reported for the synthesis of FGMs; such as plasma spraying, centrifugal casting, powder technology, PVD, CVD, and colloidal processing. Amongst these processes, electrophoretic deposition (EPD) is a fairly rapid low cost process, capable of manufacturing continuously graded materials with complex geometry [5]. The powder technology process proofs flexible and suitable route for FGM fabrication. A common practice is to build-up of the graded structure by a stepwise composition of precursor materials or powders. The manufacturing process of a FGM can usually be divided in two major steps. The first step is the construction of spatially distributed structure of constituent materials which is called the gradation. Then, transform to bulk material via the consolidation of the constituents by e.g. an appropriate sintering process [6].

An emerged sintering technique called Spark Plasma Sintering SPS gains much attention in the scientific community. A pulsated electrical energy is provided to the powder compact which is momentarily energize it and generates spark plasma. Thus, sinter bonding of the particles is stimulated across the compact. Repetitive pulses in the course of 5 to 20 minutes accomplish sintering including temperature

rise and holding time. Consequently, the SPS process is carry out in relatively short period. Other advantages of the SPS process are that it not accompanied with heating of the compact surrounding and consumes much less energy compared with conventional sintering.

In SPS process, the powder compact is usually contained in a graphite die which acts as the sintering mold and the heating element. As the graphite die conveys the electrical energy, the high thermal energy efficiency of the process is due to the direct heating of the powder compact by large spark pulse current. This heating mechanism also helps in producing homogeneous and high quality sintered compact [7].

Alumina-Titanium functionally graded materials found sound thermomechanical applications in aircraft structures [8,9]. FGM reduces the thermal stresses, residual stresses, and stress concentrations found in traditional composites. The aim of this work is study the synthesis of this material via the spark plasma sintering and the effect of different sintering conditions on the final sintered density of this type of graded material.

EXPERIMENTAL PROCEDURE

The starting materials in this work were Al_2O_3 powder (Albemarle Corporation-Germany, purity 99.8 % and average particle size 1.5µm) and TiH_2 (ABCR company-Germany, purity 99% and average particle size 1.5µm). The Titanium hydride is chosen as source of Ti metal because it is a cheaper source of Ti. In addition, it is used to avoid oxidation problem of the metal in ordinary lab conditions. TiH_2 readily decomposes to Ti at approximately 600°C throughout the SPS process. The starting materials were provided by the Department of Materials Science and Technology-Bergakademie Technical University-Freiberg-Germany. The whole experimental part is gratefully carried out at their laboratories.

The green compacts are prepared from five layers starting from 100wt% Al_2O_3. The other layers composed of 75wt%, 50wt%, 25wt% and 0wt% of Al_2O_3 respectively. The remaining weight percentages are for TiH_2. I.e. the green compacts have five layers. The first is totally Al_2O_3, the last layer is totally TiH_2, and the in-between layers are stepwise changing mixes of the two chemical compound. Carful mixing procedure is followed to ensure homogenous powder mixes (Pulverisette 6 Planetary programmable Mono Mill - Fritsch Company, Germany is utilized). The layer thicknesses (also called FGM profile) are arranged to be 1, 2, 3, 4 and 5 mm respectively. The thickness is controlled via preliminary investigation of the green density and weight calculations. Accordingly, the total high of the FGM specimen was 15 mm.

A graphite die is utilized to prepare the powder compacts. The employed die height is 48mm (figure 1-a), the inner diameter is 12mm and the outer diameter is 40mm. The heights of the upper and lower punches are 35mm. Each punch has a hole utilized to convey electrical energy on SPS. Tow accessory graphite cupfuls is also shown in the figure that is used to fix two axial pyrometers to measure SPS temperature. In order to prevent any graphite contamination during sintering process, a texture paper (figure 1-b) is used as a sealing material.

The graphite die was externally covered with graphite wool to hinder thermal radiation to the lab environment (figure 2-a). Simultaneous compaction (with 100 kg compaction force) and DC pulses are performed to the FGM compacts to accomplish the SPS process. The SPS device is (HPPD-Germany) is shown in figure 2-b. The device allows programmable control of the process parameters; i.e. the sintering time and temperature and the applied compaction force throughout sintering.

The apparent densities of the sintered samples were measured using Archimedes method. Calculations of the theoretical densities for the full dense FGM were based on mixture rules as demonstrated by Miyamoto et al [1]; The obtained theoretical densities of the FGM's were utilized in the calculations of the porosity percentages for the prepared FGM's; which is based on the difference of the theoretical and apparent densities.

The percentages of the diametrical change after SPS sintering of the FGM's were also measured to further characterize the sintered specimens. The microstructure was observed with an optical microscope (Neophot 30/carl zelss - JENA Company - Germany). The microscope was equipped with A4i analysis computer program to obtain the image with best resolution.

RESULTS AND DISCUSSION

Due to limited availability of SPS experiments, two samples are sintered at the same temperature (1400°C) and compaction force (5kN) with different sintering dwell time (10 and 15 min). Another two samples are sintered with constant dwell time (15 min) and constant compaction force (8 kN) but with different sintering temperature (1400 and 1500°C). The last two samples are sintered with the same sintering temperature (1500°C) and compaction force (8 kN) but with different dwell time (20 and 30 min). The parameters of the performed sintering experiments are shown in table (1).

Figure (3-a) shows the apparent density versus sintering time for FGM compacts sintered at 1400°C and compacting pressure of 5kN. The higher sintering time give higher apparent density. The higher compaction force (8kN) with same temperature and sintering time of 15 minutes also give higher density. This can be seen at the first column of figure (3-b) compared with the second column of figure (3-a). In addition, figure (3-b) shows that sintering at higher temperature (1500°C) results in higher density. Looking at figure (3-c), once more the higher sintering time gives higher density.

As shown in figure (3); the highest density recorded with this work (4.25g.cm^{-3}) is that with the higher sintering time and temperature and the higher compaction force. Two competitive processes are taken place throughout the SPS process. The first is the release of H_2 gas upon conversion of TiH_2 to elemental Ti. This process should enhance generation of vacancies in the sintered bulk of the materials. The other process is the enhancing of the vacancy diffusion at higher sintering temperature and better propagation of vacancies with higher sintering time. These effects derive the resultant densities for higher values.

The above discussion shows that the porosity elimination enhances the resultant densities. Explicitly, the density and the porosity complementary, which is the conclusion that can be drawn from figure (4). This figure shows the correspondent porosity percentages for the sintered compacts shown in figure (3). Similarly, the best (lower) percentage of porosity is found with SPS specimens at the higher compaction force, sintering time and sintering temperature.

The results for diametric variation after SPS process shows diametric expansion for the sintered specimens as shown in figure (5). The same conclusion can be drawn in that lower diametrical expansions were shown with higher compaction forces, higher sintering time and higher sintering temperature. The origin of the diametrical expansion can be approached from the expansion pressure originated from the H_2 release. Lateral expansion is not noticed due to the axial compaction force throughout the SPS process. The behavior of that expansion is that it shows lower values with lower porosities and higher densities. I.e. the vacancy diffusion and propagation that led to higher sintered densities and lower porosities assist reduction of the diametrical expansion.

Figure (6) shows the microstructure of a prepared FGM (FGM-6 in table 1). The upper layer of part-a is a bright area representing titanium metal. Some porosity is shown by the dark spots which ought to the liberation of H_2 from TiH_2 throughout the SPS process. A smeared interface is then follows as entrance to the second layer. A 25%wt of Al_2O_3 is introduced in the second layer which appears as dark component in the microstructure due low reflectivity of the optical light from ceramics.

Part-b of figure (6) shows an upper part of FGM layer composed of 25wt% Al_2O_3 and 75wt% Ti again. The lower layer is composed of 50wt% Al_2O_3 and 50wt% Ti. Thus, the region of lower layer appears darker. A clearer interface is shown but it still reflects dispersed material across it. The lower layer at part-b is the upper layer at part-c for figure (6). The Al_2O_3 content is incremented from 50wt% at the upper layer to 75wt% at the lower layer of part-c of the figure. The interface is more explicit but so far, it shows spreading of the ceramic and metal phase and no abrupt change. The last part-d of figure (6) show upper layer composed of 75wt% Al_2O_3 and 25wt% Ti. While the lower layer shows 100% Al_2O_3 region. The interface is visually more distinct because it reflects transform from two phase region to single (dark) phase region.

Examination of micrographs of higher magnification at figure (7) reveals abundant bridging between the upper and lower layer for all the interfaces. Darker spots are shown in the ceramic region which reflects the left porosity after the sintering process. A general conclusion is drawn from figures (6-7) is that the specimen is composed of five graded layers with interfaces that reveals interconnecting and gradual change in composition, thus, strong bonding is expected between the two layers. These results are in coherence with previous review of processing techniques of FGM [6] and a previous study of SPS parameters [7]. As mentioned earlier, Al_2O_3-Ti system has sound thermomechanical properties; for that reason, this study contribute in the introducing the SPS of that system. The role of SPS compared with other sintering method is its inherent process speed that

exclude the need for vacuum sintering and its allows for applying constant pressure in the duration of sintering that helps reducing porosity and enhancing density of the product.

CONCLUSIONS

1. **Stepwise Al_2O_3-Ti functionally graded specimens have been constructed starting from Al_2O_3-TiH_2 powder mixes and compaction to produce powder compacts of graded composition. TiH_2 is converted to metal Ti during sintering.**
2. **Spark plasma sintering is successfully applied to the green specimens. Higher sintering time, temperature, and higher compaction force gives lower porosity and diametrical expansion.**
3. **Optical microscopy shows smeared interfaces between the graded layers which reflects good adaptation and gradation of FGM layers.**

REFERENCES

[1]. Kaysser, M. Y., W.A., Rabin B.H., Kawasaki A. and Ford R.G. "Functionally graded materials design, processing and applications", Kluwer Academic Publishers, 1999.

[2]. Yaghoobi, H. and Feridoon A., "Influence of neutral surface position on deflection of functionally graded beam under uniformly distributed load", world applied science journal, vol 10(3), pp 337-341, 2010.

[3]. Kudesia, R., Niedzialek S. E., Stangle G. C., McCauley J. W., Richard M. and Kaieda Y., "Design and fabrication of TiC/NiAI functionally gradient materials for joining applications", 16th Annual conference on composites and advanced ceramic materials, vol.13, issue 7/8, edited by John B. Wachtman, pp.٣٨٣-٣٧٤ , Wiley, 2010.

[4].Birman, V., Byrd L. W., "Modeling and Analysis of Functionally Graded Materials and Structures", Appl. Mech. Rev. vol. 60, pp.195-216, 2007.

[5]. Put, S., Vleugels J. and Van der Biest O., "Microstructural engineering of functionally graded materials by electrophoretic deposition", Journal of materials processing technology, vol 143-144, pp 572-577, 2003.

[6]. Kieback, B., Neubrand A., Riedel H. "Processing techniques for functionally graded materials", Mat. Sci. Eng. vol: A362, pp.81–105, 2003.

[7]. Munir, Z. A., Anselmi-Tamburini U, Ohyanagi M., "The effect of electric field and pressure on the synthesis and consolidation of materials: A review of the spark plasma sintering method", J mater sci. vol.41, pp.763–777, 2006.

[8]. Cooley, W. G., "Application of functionally graded materials in aircraft structures", Thesis, Department of the air force, Air University, USA, 2005.

[9]. Hao Y. X., Zhang W., and Ji X. L., "Nonlinear Dynamic Response of Functionally Graded Rectangular Plates under Different Internal Resonances," Mathematical Problems in Engineering, vol. 2010, Article ID 738648, 12 pages, 2010.

Table (1): The parameters of the performed SPS

Symbol	Sintering Temperature □ C	Sintering Dwell Time min	Compaction Force kN
FGM-1	**1400**	**10**	**5**
FGM-2	**1400**	**15**	**5**
FGM-3	**1400**	**15**	**8**
FGM-4	**1500**	**15**	**8**
FGM-5	**1500**	**20**	**8**
FGM-6	**1500**	**30**	**8**
Heating rate: 50°C/min, Cooling rate: 45°C/min			

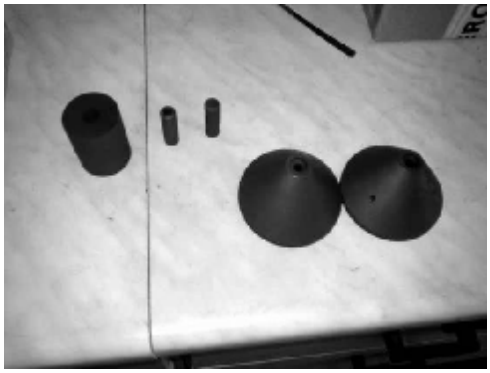

-a-

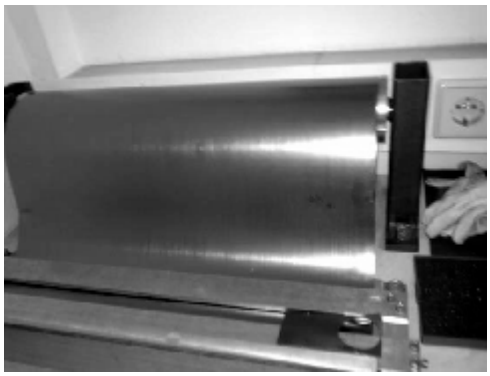

-b-

Figure (1): a- the graphite dies, b- graphite texture paper.

-a- **-b-**

Figure (2): a- The graphite die insulated with graphite wool, b- The SPS apparatus.

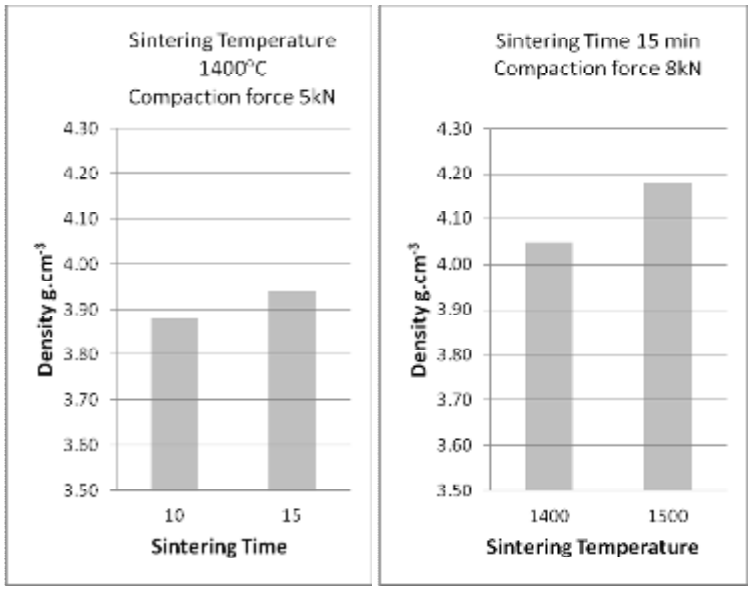

a **b**

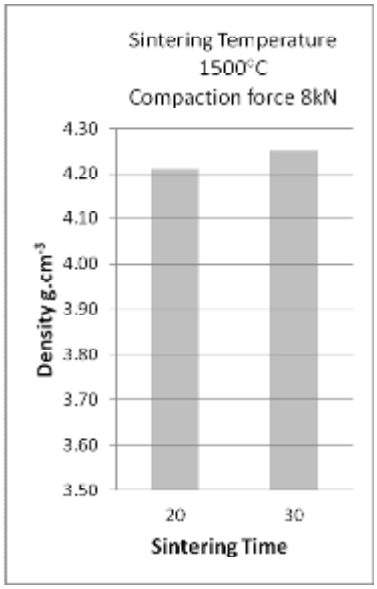

c

Figure (3): Density for SPS sintered compacts for different sintering conditions:
a- Sintering Temperature 1400°C, Compaction force 5kN.
b- Sintering Time 15 minute, Compaction force 8kN.
c- Sintering Temperature 1500°C, Compaction force 8kN.

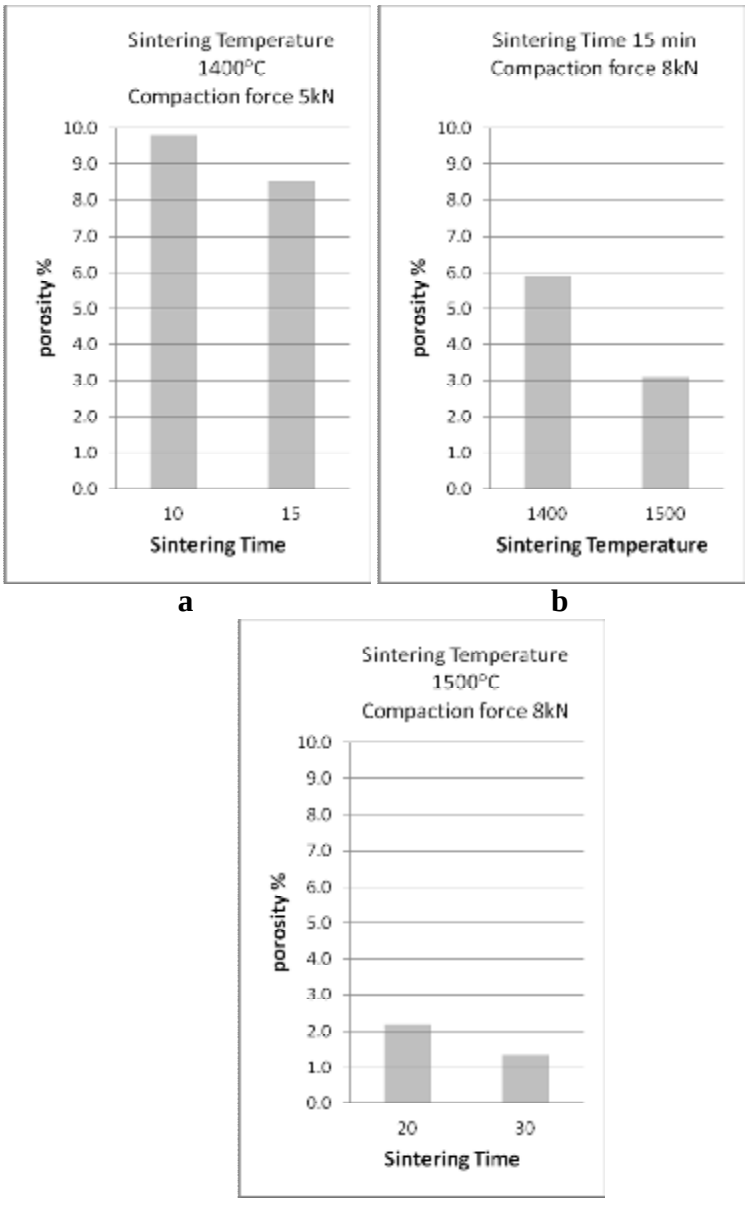

Figure (4): porosity% for SPS sintered compacts for different sintering conditions:

a- Sintering Temperature 1400°C, Compaction force 5kN.
b- Sintering Time 15 minute, Compaction force 8kN.
c- Sintering Temperature 1500°C, Compaction force 8kN.

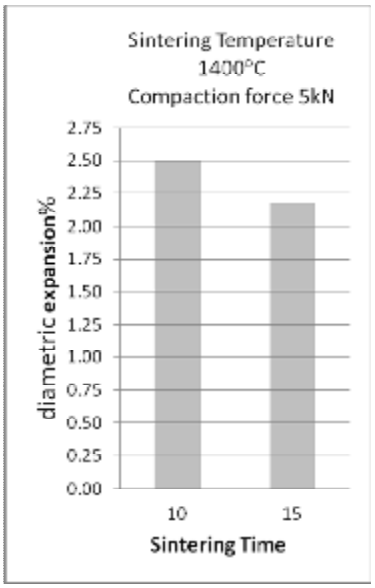

a

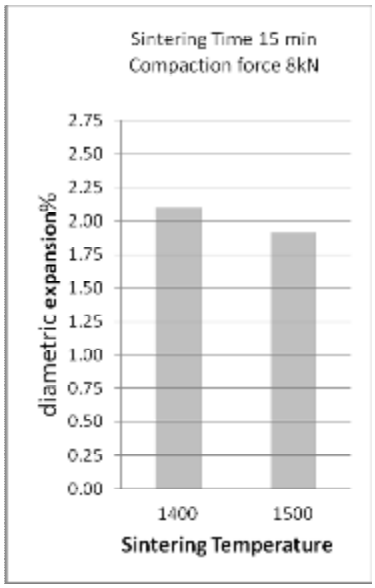

b

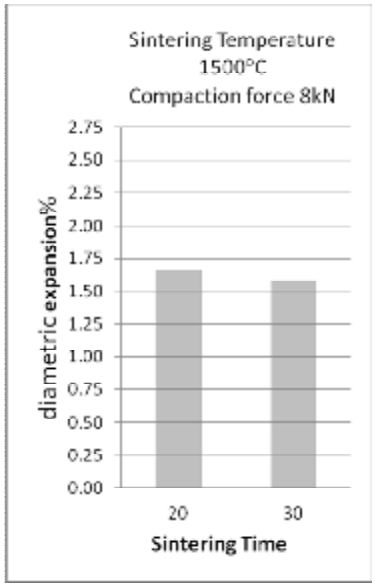

a c

Figure (5): Density for SPS sintered compacts for different sintering conditions:
a- Sintering Temperature 1400°C, Compaction force 5kN.
b- Sintering Time 15 minute, Compaction force 8kN.
c- Sintering Temperature 1500°C, Compaction force 8kN.

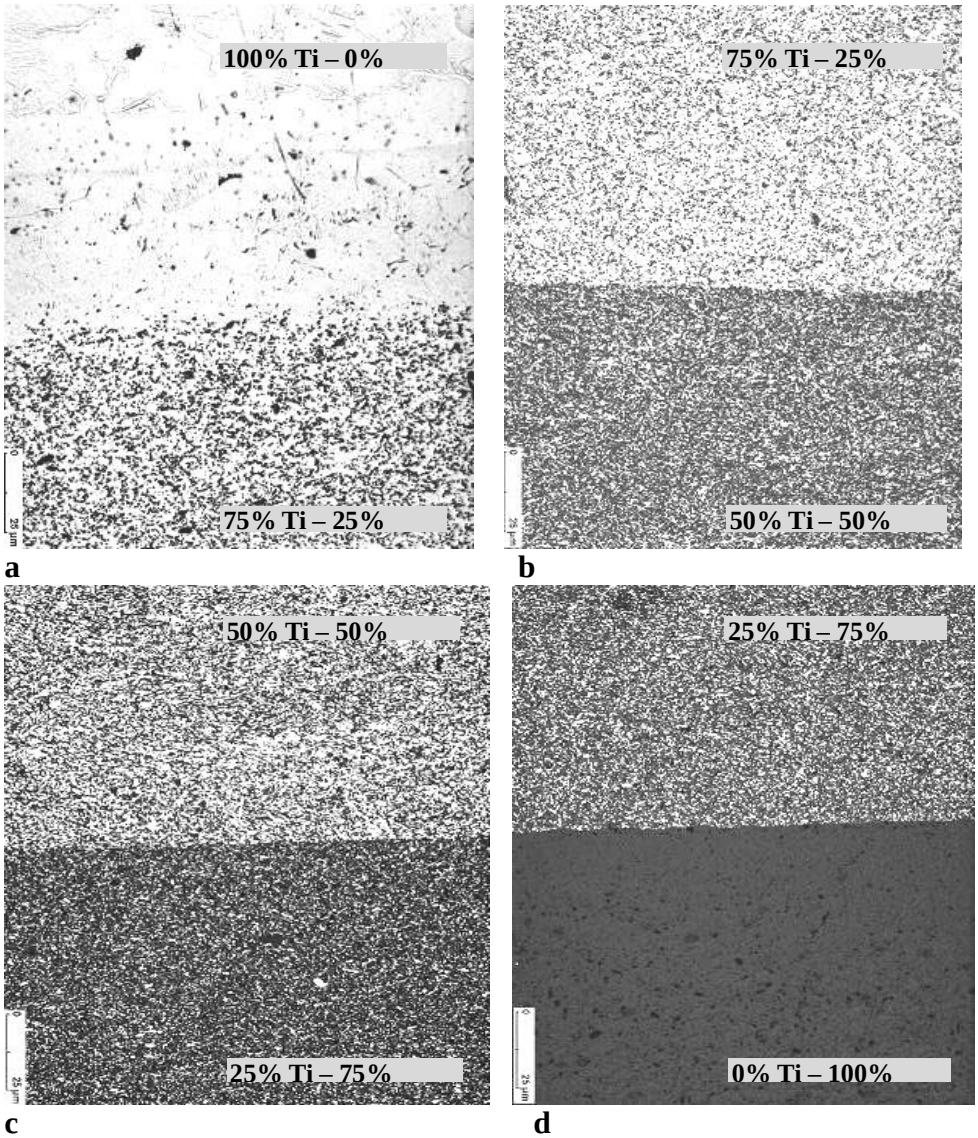

Figure (6): Optical micrographs for the FGM's showing the interface between five different layers (Scale Bar=25mm); the upper layer and lower layers are:

- **a- 100% Ti – 75% Ti.**
- **b- 75% Ti – 50% Ti.**
- **c- 50% Ti – 25% Ti.**
- **d- 25% Ti – 0% Ti (100% Al_2O_3).**

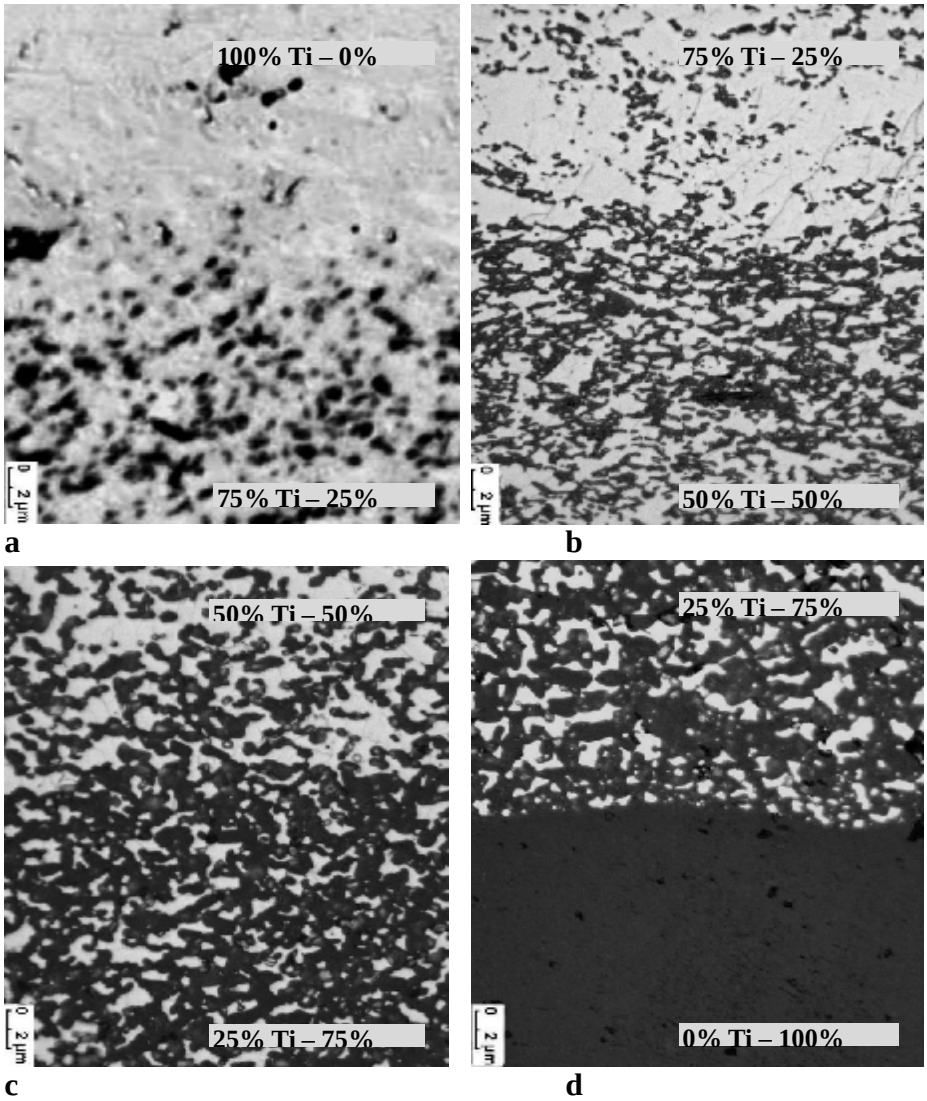

Figure (7): Optical micrographs for the FGM's showing the interface between five different layers (Scale Bar=2㎜); the upper layer and lower layers are:

a- 100% Ti – 75% Ti.
b- 75% Ti – 50% Ti.
c- 50% Ti – 25% Ti.
d- 25% Ti – 0% Ti (100% Al_2O_3).